NANO LETTERS

2007
Vol. 7, No. 6
1570−1574

Direct Observation of the Structural Component of the Metal–Insulator Phase Transition and Growth Habits of Epitaxially Grown VO_2 Nanowires

Jung Inn Sohn,[†] Heung Jin Joo,[†,‡] Alexandra E. Porter,[†] Chel-Jong Choi,[§] Kinam Kim,[‡] Dae Joon Kang,[†,||] and Mark E. Welland*,[†]

Nanoscience Centre, University of Cambridge, Cambridge CB3 0FF, United Kingdom, ATD Team, Memory Division, Semiconductor Business, Samsung Electronics Co., Yongin City, Korea, Future Technology Research Division, Electronics and Telecommunications Research Institute (ETRI), Daejeon 305-700, Korea, BK 21 Physics Research Division, SKKU Advanced Institute of Nanotechnology (SAINT) and Center for Nanotubes and Nanostructured Composites (CNNC), Sungkyunkwan University, Suwon 440-746, Korea

Received February 23, 2007; Revised Manuscript Received April 24, 2007

ABSTRACT

We have grown epitaxially orientation-controlled monoclinic VO_2 nanowires without employing catalysts by a vapor-phase transport process. Electron microscopy results reveal that single crystalline VO_2 nanowires having a [100] growth direction grow laterally on the basal *c* plane and out of the basal *r* and *a* planes of sapphire, exhibiting triangular and rectangular cross sections, respectively. In addition, we have directly observed the structural phase transition of single crystalline VO_2 nanowires between the monoclinic and tetragonal phases which exhibit insulating and metallic properties, respectively, and clearly analyzed their corresponding relationships using in situ transmission electron microscopy.

One-dimensional (1D) nanoscale building blocks based on functional nanowires and nanotubes are of considerable interest for their potential applications in electronic, optical, optoelectronic, and piezoelectric nanodevices due to the structural versatility and unique chemical and physical properties.[1−5] In order to realize these applications, the precise control over position and orientation of building blocks on substrates is of great importance since these will define physical properties and integrate 1D building blocks into a designed system. Thus, to achieve this goal, several strategies have been developed using different fabrication methods, e.g., electric field assisted assembly techniques, use of microfluidic channels, the Langmuir−Blodgett technique, and the "pick and place" technique.[6−10] Alternatively, other strategies based on in situ growth have been developed to control the orientation of building blocks directly onto the desired position on the appropriately selected substrates by defining the position of the catalysts or seed layers.[11−14] However, these approaches require sophisticated techniques or/and catalysts to control position and orientation of building blocks. These are of serious impediment to the practical fabrication process as well as to the device performance due to the slow and inefficient process and because of contamination resulting from the fabrication process and the presence of catalysts.[15,16] Thus, an ideal and simple way to avoid these problems is epitaxial growth of nanowires directly on device substrates along a chosen crystallographic growth direction without introducing catalysts.

On the basis of the conventional epitaxial crystal growth technique, so far, numerous studies on epitaxial growth of inorganic nanowires have been performed to achieve orientation-controlled single crystalline inorganic nanowires for the exploration of fundamental physics as well as for their novel applications complementary to the bulk materials. Among the various inorganic nanowires studied to date,[1−9,12−20] VO_2 nanowires have attracted great attention because of their metal to insulator transitions and reversible dramatic changes in electrical and optical properties accompanied by a

* Corresponding author: e-mail, mew10@cam.ac.uk; tel, 44-1223-760305; fax, 44-1223-760306.
[†] Nanoscience Centre, University of Cambridge.
[‡] ATD Team, Samsung Electronics Co.
[§] Future Technology Research Division, ETRI.
[||] BK21 Physics Research Division, SAINT, CNNC, Sungkyunkwan University.

10.1021/nl070439q CCC: $37.00
Published on Web 05/18/2007

structural phase transition.[21−23] These properties of VO_2 make it a promising material for the use in device applications to achieve reliable switching operations in the nanometer scale regime. Despite these attractive features and a few recent reports on the growth of nanoscale VO_2,[1,19,20] to the best of our knowledge, there are no reports on orientation-controlled single crystalline epitaxial growth of 1D monoclinic VO_2, probably due to difficulties of growth associated with the presence of various competing vanadium oxide phases and rotational symmetry.[24−26] Further, there are no detailed accounts describing the growth characteristics of VO_2 nanowires and the relationship of the structural phase transitions between monoclinic and tetragonal rutile structures that exhibit insulating and metallic properties, respectively.

In this paper, we report a simple vapor-phase transport process based on epitaxial growth to control the orientation of single crystalline VO_2 nanowire arrays with distinct morphology. We demonstrate that single crystalline monoclinic VO_2 nanowires having a [100] growth direction grow laterally on *c*- and away from the planes of *r*- and *a*-cut single-crystal sapphire substrates with the low-energy $(01\bar{1})$ and (011) side facets, exhibiting triangular and rectangular cross sections, respectively. A clear understanding of growth characteristics of VO_2 nanowires and the relationship of the phase transitions between monoclinic and tetragonal structures showing a reversible transition are crucial for controlling their properties and designing devices made from them. For this reason, we investigated growth characteristics of nanowires and directly observed the structural component of the reversible phase transition using in situ transmission electron microscopy (TEM).

Single crystalline VO_2 nanowires were grown on *c*-cut (0001), *r*-cut $(\bar{1}012)$, and *a*-cut $(11\bar{2}0)$ single-crystal sapphire substrates under identical growth conditions using a vapor-phase transport process[2] without employing any metal catalysts. Substrate and VO_2 powder were placed in an alumina boat. The boat was inserted into an alumina reaction tube, which was placed in a high-temperature tube furnace. Prior to the growth, the alumina tube was first pumped down to a pressure of less than 10 mTorr. Argon (Ar) as the carrier gas for the vapor reactants was then introduced into the reaction tube at a flow rate of 50−100 sccm while the furnace was heated at a rate of 30 °C/min under 5−10 Torr pressure. The growth temperature and time were 600−700 °C and 2−5 h, respectively. After the growth process was completed, the samples were naturally cooled to room temperature in an Ar gas ambient. Scanning electron microscopy (SEM, LEO 1530 VP) was used to characterize the surface morphology and orientation of the nanowires, and high-resolution transmission electron microscopy (HRTEM, Tecnai G2 F20) was employed to assess the growth direction and crystal structure of the nanowires. In situ convergent beam experiments were performed to observe the phase transition from monoclinic to tetragonal crystal structures during the heating.

Figure 1a shows an SEM image of epitaxially grown VO_2 nanowires on a *c*-cut sapphire substrate. The VO_2 nanowires grow laterally on the basal plane along the $\langle 11\bar{2}0\rangle$ directions of *c*-cut sapphire substrates, which were cleaved to effect

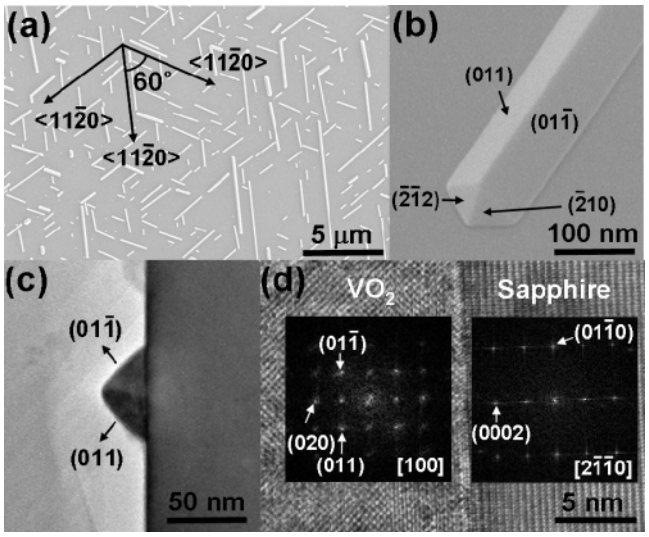

Figure 1. Single crystalline VO_2 nanowires grown on the *c*-cut sapphire substrates. (a) A typical SEM image of VO_2 nanowires grown laterally along the three equivalent $\langle 11\bar{2}0\rangle$ directions of sapphire. (b) A high-magnification SEM image, showing the morphology of a VO_2 nanowire with well-defined surfaces at both a tip and a side. (c) A cross-sectional TEM image obtained from the interface between a VO_2 nanowire and a sapphire substrate and (d) the corresponding FFT pattern indexed to monoclinic VO_2. These results reveal that a VO_2 nanowire grown along a [100] direction exhibits a triangular cross section consisting of bounding $(01\bar{1})$ and (011) side facets and a (010) bottom surface.

growth orientation along the $[11\bar{2}0]$ direction before the epitaxial growth. The angles between nanowires are either 60° (and/or 120°) or parallel to each other. This finding provides the strong evidence that nanowires grew preferentially along the three equivalent $\langle 11\bar{2}0\rangle$ directions of the sapphire rotated by 120° on the basal *c* plane. The high-magnification SEM image shows that the VO_2 nanowires are well faceted at both the tip and side surfaces, as shown in Figure 1b. This implies that the bounding facets of VO_2 nanowires formed during the epitaxial growth have low-energy surfaces compared to other planes of VO_2.

To characterize the growth direction and crystal structure of VO_2 nanowires, TEM examinations were carried out. Parts c and d of Figure 1 show a cross-sectional TEM image from an interface region of the sample grown laterally on a *c*-cut sapphire substrate and the corresponding 2D fast Fourier transform (FFT) patterns, respectively. These results reveal that the VO_2 nanowire grown on a *c*-cut sapphire substrate exhibits a triangular cross section consisting of bounding $(01\bar{1})$ and (011) side facets and a (010) bottom surface. Furthermore, the FFT patterns indexed to monoclinic VO_2 confirm that the epitaxial relationship between a VO_2 nanowire and *c*-cut sapphire is (010) VO_2//(0001) sapphire, which is consistent with thin film results previously reported by other groups.[24,25] It is noteworthy that the vertical direction of the cross section of VO_2 nanowires is perpendicular to the $\{11\bar{2}0\}$ sapphire plane, showing that the growth direction of VO_2 nanowires is parallel to the $\langle 11\bar{2}0\rangle$ directions of sapphire. This indicates that VO_2 nanowires having a [100] growth direction can be preferentially grown with the bounding $(01\bar{1})$ and (011) side facets, which are low-index

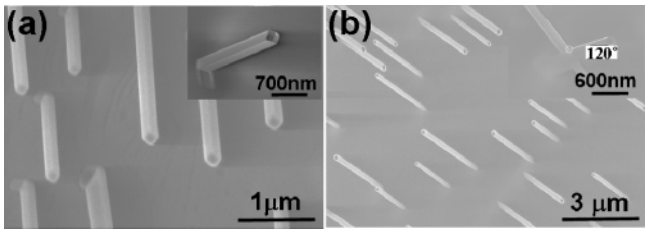

Figure 2. Typical SEM images of the VO_2 nanowires grown on (a) *r*-cut and (b) *a*-cut sapphire substrates. It is noted that the growth directions of VO_2 nanowires are directly affected by the crystallographic planes of the sapphire substrates.

crystallographic planes and low-energy surfaces,[19,26] on the basal *c* plane along three equivalent $\langle 11\bar{2}0\rangle$ directions of sapphire on the basal *c* plane, which is in excellent agreement with the SEM results shown in parts a and b of Figure 1, exhibiting three unique growth directions of VO_2 nanowires with well-defined facets.

Figure 2 shows SEM images of VO_2 nanowires epitaxially grown on *r*- and *a*-cut sapphire substrates. In contrast to nanowires grown on a *c*-cut sapphire substrate, for the *r*- and *a*-cut sapphire substrates, VO_2 nanowires grew out of the basal *r* and *a* planes of sapphire shown in parts a and b of Figure 2, respectively. VO_2 nanowires also grew into regular arrays with unique growth direction and angle between their growth axes and the basal plane. It is noted that VO_2 nanowires form an angle of 60° with respect to the basal *r*-cut sapphire substrate, as shown in the inset of Figure 2a, and are either parallel or 120° to each other on the *a*-cut sapphire substrate, as shown in the inset of Figure 2b. This finding suggests that, for the growth of VO_2 nanowires without catalysts, the growth direction of VO_2 nanowires is directly affected by the orientation of the plane of sapphire substrates. This observation provides strong evidence of single crystalline epitaxial growth of VO_2 nanowires associated with the lattice match between nanowires and substrates, symmetry, and the formation of crystal planes with low energy.

The growth direction and crystal structure of VO_2 nanowires grown on the *r*-cut sapphire substrate can be clearly verified by TEM and high-magnification SEM images of nanowires. (It should be noted that TEM results show no differences in growth directions and crystal structure between nanowires grown on *r*- and *a*-cut sapphire substrates, respectively.) A low-magnification TEM image of a representative VO_2 nanowire and a selected area electron diffraction (SAED) pattern taken from the same sample are shown in Figure 3a. A SAED pattern taken along the [122] zone axis indicates that a VO_2 nanowire is a single crystalline monoclinic structure with a [100] growth direction, which is perpendicular to a $(\bar{2}01)$ growth front plane and is enclosed by $\{01\bar{1}\}$ and $\{011\}$ side planes forming a rectangular cross section. These growth characteristics and crystal structures of VO_2 nanowires are similar to those of nanowires grown on *c*-cut sapphire substrates except that all nanowires have rectangular cross sections due to the different orientation relationships at interfaces.

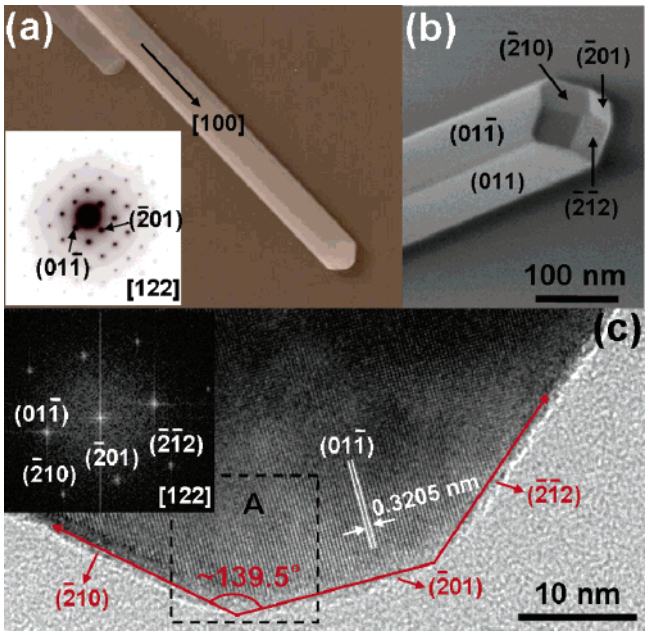

Figure 3. Single crystalline VO_2 nanowires grown on the *r*-cut sapphire substrates. (a) A low-magnification TEM image of a representative VO_2 nanowire and the SAED pattern taken from the same sample, which confirm that VO_2 nanowires are single crystal of the monoclinic structure growing along the [100] direction. (b) A high-magnification SEM image of VO_2 nanowires with prismatic tips and rectangular cross sections. (c) A HRTEM image of a tip of VO_2 nanowires, showing exactly a $(01\bar{1})$ side plane parallel and a $(\bar{2}01)$ growth front plane perpendicular to a [100] growth direction.

Figure 3c shows that a HRTEM image of a tip of VO_2 nanowires clearly reveals lattice fringes, indicating that a VO_2 nanowire is single crystalline. The lattice spacing of adjacent planes is about 0.3205 nm corresponding to that between the $(01\bar{1})$ planes of monoclinic VO_2, showing that nanowires grow along the [100] direction parallel to a $(01\bar{1})$ plane and perpendicular to a $(\bar{2}01)$ plane. This result is in exact agreement with the FFT pattern shown in the inset of Figure 3c as well as the SAED pattern shown in Figure 3a. It can be also seen that nanowires terminated by a prismatic form, as shown in Figures 3b and 1b, have a $(\bar{2}01)$ growth front plane, $(01\bar{1})$ and (011) side planes, and $(\bar{2}10)$ and $(\bar{2}\bar{1}2)$ intersection planes between $(\bar{2}01)$ and $(01\bar{1})$ plane and (011) plane, respectively. In addition, the structural orientation between intersection planes and a $(\bar{2}01)$ plane is in agreement with measured values from Figure 3c. Note that the difference of surface energies among various crystal planes leads to their different growth rates. In other words, the growth of crystal planes with low energy proceeds slowly, whereas crystal planes with high energy grow fast, leaving behind slowly growing planes, namely, low-energy planes.[27,28] Thus, a prismatic shape of nanowires shown in Figures 1b and 3b is believed to be attributed to the relative growth rates of $(\bar{2}01) > (\bar{2}10)$ and $(\bar{2}\bar{1}2) > (01\bar{1})$ and (011) planes.

A comparison of the SEM and TEM results shows that single crystalline VO_2 nanowires could be grown along the [100] direction with a unique growth orientation relationship with respect to the planes of sapphire substrates by taking advantage of low index crystallographic facets, such as $(01\bar{1})$

and (011) planes, and the good heteroepitaxial interface between VO_2 and sapphire planes. Hence, since the *c* plane of sapphire is inclined 57.6° and 90° to *r* and *a* planes of sapphire, respectively, single crystalline epitaxial growth along the [100] direction of VO_2 nanowire may be achieved by tilting from *r* and *a* planes of substrates. Here, it is important to note that we can achieve orientation-controlled single crystalline VO_2 nanowires in contrast to thin film VO_2 single crystals, which have proven difficult to grow due to the presence of various competing oxide phases and rotational symmetry causing the formation of twin or polycrystalline boundaries.[24−26]

The vapor−solid (VS) and the vapor−liquid−solid (VLS) mechanisms have been proposed to explain the formation process of 1D nanomaterials.[2−3,29−31] In our study, no metal catalysts were used and no metal droplets appeared at the tip of each nanowire after its growth. Even though the growth mechanism is still unclear, it is likely that the growth of VO_2 nanowires follows the VS mechanism. This growth characteristic of VO_2 nanowires may be explained as follows. Source materials are vaporized at growth temperature and transported from the gas phase to the sapphire substrate by the Ar inert gas stream. Then, vapor reactants are adsorbed at an appropriate site through the close-packed arrangements of oxygen atoms between the (010) VO_2 and the (0001) sapphire substrate shown in Figure 1d, followed by the arrangements of cations such as Al and V in different interstices of the close-packed oxygen network.[25] After completion of an initial stage of epitaxial growth for the formation of single crystalline VO_2 nanowires, VO_2 tends to maximize the areas of $(01\bar{1})$ and (011) facets due to the low-energy surface along the [100] direction,[19,26] which is the preferred growth direction of VO_2 nanowires. It seems that the minimization of surface energy may play an important role in controlling the growth habit and formation of nanowires.[2,27,28] Also important to note is the prismatic shape of growth fronts shown in Figures 1b and 3b, probably attributed to the relative growth rate of $(\bar{2}01) > (\bar{2}10)$ and $(\bar{2}\bar{2}12) > (01\bar{1})$ and (011) planes. This is consistent with the growth habit of crystal determining a crystal shape and a growth direction. Hence, epitaxial growth of nanowires with the preferred growth direction and orientation without introducing catalysts can be explained in terms of the minimization of surface energy and lattice match during the crystal growth.

A phase transition between monoclinic and tetragonal VO_2 phases showing a reversible transition[26] would be crucial for achieving abrupt changes in electrical and optical properties. For this reason, we characterized the structural phase transitions of single crystalline VO_2 nanowires using in situ TEM. TEM samples were prepared by the dispersion of VO_2 nanowires grown on *r*-cut sapphire substrates on a Cu grid covered with holey carbon. The temperature of the sample holder with heating stage is measured by a thermocouple that is adjacent to but not directly measuring the actual sample. To ensure that the sample temperature was as close as possible to the measured temperature, we therefore waited for 1 h for thermal equilibriation. Parts a and b of Figure 4

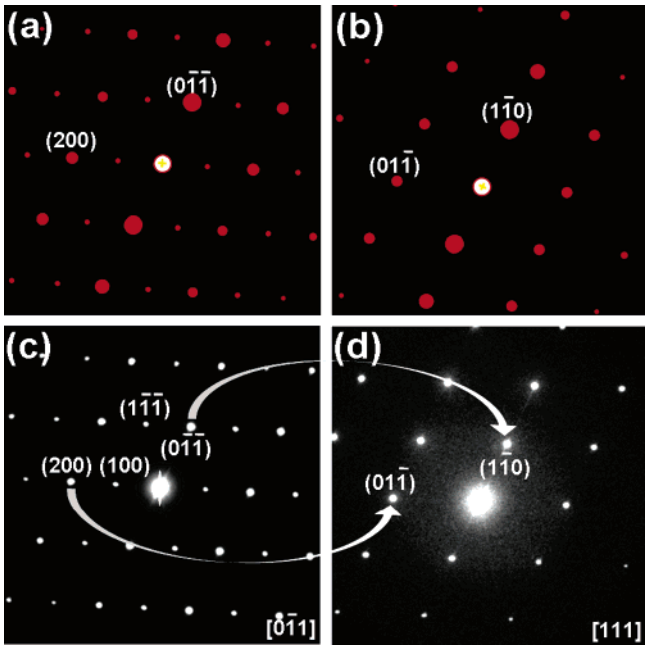

Figure 4. The calculated diffraction patterns (a) for a $[0\bar{1}1]$ zone axis in a monoclinic structure of VO_2 and (b) for a [111] zone axis in a tetragonal structure of VO_2. (c and d) Corresponding SAED patterns of VO_2 nanowires obtained at room temperature and 70 °C, respectively.

show calculated diffraction patterns for a $[0\bar{1}1]$ zone axis in a monoclinic structure and a [111] zone axis in a tetragonal structure, while the corresponding convergent beam patterns of VO_2 nanowires obtained at room temperature and 70 °C are shown in parts c and d of Figure 4, respectively. The values used in this calculation are obtained from refs 32 and 33. It is shown that the intensity and position of experimental diffraction patterns obtained at low and high temperatures are in good agreement with those of calculated monoclinic and tetragonal diffraction patterns, respectively. Also, note that a zone axis of $[0\bar{1}1]$ in a monoclinic structure corresponded to that of [111] in a tetragonal structure. This demonstrates that the phase transition from a monoclinic to a tetragonal structure has occurred during the heating. After the sample was cooled to room temperature, the same convergent beam patterns as those shown in Figure 4c appeared again. This result shows that phase transitions are reversible. The detailed relationship of diffraction patterns between monoclinic and tetragonal structures can be explained as follows. All diffraction patterns could be indexed on the basis of a monoclinic structure related to a tetragonal structure by a transition matrix given by as[32]

$$\begin{pmatrix} a \\ b \\ c \end{pmatrix}_{\text{monoclinic}} = \begin{pmatrix} 0 & 0 & -2 \\ -1 & 0 & 0 \\ 0 & 1 & 1 \end{pmatrix} \begin{pmatrix} a \\ b \\ c \end{pmatrix}_{\text{tetragonal}}$$

It is noted that $(0\bar{1}\bar{1})$ and (200) planes in a monoclinic structure become $(1\bar{1}0)$ and $(01\bar{1})$ planes in a tetragonal structure, respectively, through the phase transition. However, spots with weak intensity such as (100) and $(1\bar{1}\bar{1})$ disappeared, indicating that those spots cannot be indexed on spots

of a tetragonal structure with [111] zone axis. It is clear from the intensity and position of diffraction spots that the phase transition from monoclinic to tetragonal structures is directly observed by in situ TEM during the heating. This finding is believed to be associated with the disappearance of the pairing and the tilting of V atoms accompanied by the phase transition, leading to the reduction in the cell as a half-size along the *c*-axis of the tetragonal structure.[32−34] To the best of our knowledge, this is the first time that using in situ TEM, the structural phase transition of single crystalline VO_2 nanowires has been directly observed and relationships of corresponding diffraction patterns have been analyzed.

In summary, we have shown that single crystalline VO_2 nanowires can be epitaxially grown along the [100] direction with a unique growth orientation relationship with respect to the planes of sapphire substrates by taking advantage of low-energy $(01\bar{1})$ and (011) facets and the good heteroepitaxial interface between VO_2 and sapphire planes, affecting their morphology including cross sections and growth directions. We also find that nanowires are terminated by a prismatic shape due to the relative growth rates of $(\bar{2}01) > (\bar{2}10)$ and $(\bar{2}\bar{1}2) > (01\bar{1})$ and (011) planes. Last, we proposed that the VS mechanism is responsible for the growth of 1D monoclinic VO_2 and directly observed its phase transition from monoclinic to tetragonal structures by in situ TEM during the heating.

Acknowledgment. This work is supported by Samsung Electronics, Korea, and the IRC in Nanotechnology. D.J.K. is supported by the SRC program of the Ministry of Science and Technology of Korea/Korea Science and Engineering Foundation.

References

(1) Patzke, G. R.; Krumeich, F.; Nesper, R. *Angew. Chem., Int. Ed*. **2002**, *41*, 2446.
(2) Dai, Z. R.; Pan, Z. W.; Wang, Z. L. *Adv. Funct. Mater*. **2003**, *13*, 9.
(3) Huang, M. H.; Mao, S.; Feick, H.; Yan, H.; Wu, Y.; Kind, H.; Weber, E.; Russo, R.; Yang, P. *Science* **2001**, *292*, 1897.
(4) Wang, Z. L.; Song, J. *Science* **2006**, *312*, 242.
(5) Lauhon, L. J.; Gudiksen, M. S.; Wang, D.; Lieber, C. M. *Nature* **2002**, *420*, 57.
(6) Smith, P. A.; Nordquist, C. D.; Jackson, T. N.; Mayer, T. S.; Martin, B. R.; Mbindyo, J.; Mallouk, T. E. *Appl. Phys. Lett.* **2000**, *77*, 1399.
(7) Harnack, O.; Pacholski, C.; Weller, H.; Yasuda, A.; Wessels, J. M. *Nano Lett*. **2003**, *3*, 1097.
(8) Huang, Y.; Duan, X.; Wei, Q.; Lieber, C. M. *Science* **2001**, *291*, 630.
(9) Whang, D.; Jin, S.; Wu, Y.; Lieber, C. M. *Nano Lett*. **2003**, *3*, 1255.
(10) Cha, S. N.; Jang, J. E.; Choi, Y.; Amaratunga, G. A. J.; Kang, D.-J.; Hasko, D. G.; Jung, J. E.; Kim, J. M. *Appl. Phys. Lett*. **2005**, *86*, 83105.
(11) Franklin, N. R.; Wang, Q.; Tombler, T. W.; Javey, A.; Shim, M.; Dai, H. *Appl. Phys. Lett*. **2002**, *81*, 913.
(12) Wang, X.; Song, J.; Li, P.; Ryou, J. H.; Dupuis, R. D.; Summers, C. J.; Wang, Z. L. *J. Am. Chem. Soc*. **2005**, *127*, 7920.
(13) Adhikari, H.; Marshall, A. F.; Chidsey, C. E. D.; Mclntyre, P. C. *Nano Lett*. **2006**, *6*, 318.
(14) Dick, K. A.; Deppert, K.; Karlsson, L. S.; Seifert, W.; Wallenberg, L. R.; Samuelson, L. *Nano Lett*. **2006**, *6*, 2842.
(15) Conley, J. F., Jr.; Stecker, L.; Ono, Y. *Appl. Phys. Lett*. **2005**, *87*, 223114.
(16) Lee, J. S.; Islam, M. S.; Kim, S. *Nano Lett*. **2006**, *6*, 1487.
(17) Choi, Y. C.; Kim, W. S.; Park, Y. S.; Lee, S. M.; Bae, D. J.; Lee, Y. H.; Park, G. S.; Choi, W. B.; Lee, N. S.; Kim, J. M. *Adv. Mater*. **2000**, *12*, 746.
(18) Zhang, Y.; Zhu, J.; Zhang, Q.; Yan, Y.; Wang, N.; Zhang, X. *Chem. Phys. Lett*. **2000**, *504*, 317.
(19) Guiton, B. S.; Gu, Q.; Prieto, A. L.; Gudiksen, M. S.; Park, H. *J. Am. Chem. Soc*. **2005**, *127*, 498.
(20) Liu, J.; Li, Q.; Wang, T.; Yu, D.; Li, Y. *Angew. Chem., Int. Ed*. **2004**, *43*, 5048.
(21) Morin, F. J. *Phys. Rev. Lett*. **1959**, *3*, 34.
(22) Wu, J.; Gu, Q.; Guiton, B. S.; Leon, N. P.; Ouyang, L.; Park, H. *Nano Lett*. **2006**, *6*, 2313.
(23) Gu, Q.; Falk, A.; Wu, J.; Ouyang, L.; Park, H. *Nano Lett*. **2007**, *7*, 363.
(24) Zhu, P.-R.; Yamamoto, S.; Miyashita, A.; Wu, Z.-P.; Narumi, K.; Naramoto, H. *Philos. Mag. Lett.* **1999**, *79*, 603.
(25) De Natale, J. F.; Hood, P. J.; Harker, A. B. *J. Appl. Phys*. **1989**, *66*, 5844.
(26) Haras, A.; Witko, M.; Salahub, D. R.; Hermann, K.; Tokarz, R. *Surf. Sci*. **2001**, *491*, 77.
(27) Wang, R. C.; Liu, C. P.; Huang, J. L.; Chen, S.-J. *Appl. Phys. Lett*. **2005**, *86*, 251104.
(28) Baxter, J. B.; Aydil, E. S. *J. Cryst. Growth* **2005**, *274*, 407.
(29) Yao, B. D.; Chan, Y. F.; Wang, N. *Appl. Phys. Lett*. **2002**, *81*, 757.
(30) Zhang, Y.; Wang, N.; Gao, S.; He, R.; Miao, S.; Liu, J.; Zhu, J.; Zhang, X. *Chem. Mater*. **2002**, *14*, 3564.
(31) Wang, L.; Zhang, X.; Zhao, S.; Zhou, G.; Zhou, Y.; Qi, J. *Appl. Phys. Lett*. **2005**, *86*, 24108.
(32) Eyert, V. *Ann. Phys. (Leipzig)* **2002**, *11*, 650.
(33) Galy, J. *J. Solid State Chem*. **1999**, *148*, 224.
(34) Wentzcovitch, R. M.; Schulz, W. W.; Allen, P. B. *Phys. Rev. Lett*. **1994**, *72*, 3389.

NL070439Q